TABLE 1. Incidences of Acute-Onset Endophthalmitis in Studies Comparing Transconjunctival Microincision Vitrectomy Surgery with Conventional 20-Gauge Vitrectomy

| Study | Centers | Study Period (yrs) | Transconjunctival MIVS | | 20-Gauge Vitrectomy | | Risk Difference (95% CI) |
			No.	(%)	No.	(%)	
Kunimoto and Kaiser,[14] 2007	1	2004 through 2006	7/3103[a]	0.226	1/5498	0.018	0.0021 (0.0004 to 0.0038)
Scott and associates,[16] 2008	7	2005 through 2006	11/1307[a]	0.842	2/6375	0.031	0.0081 (0.0031 to 0.0131)
Simada and associates,[17] 2008	1	2000 through 2007	1/3343[a]	0.030	1/3592	0.028	0.0000 (−0.0008 to 0.0008)
Chen and associates,[18] 2009	1	2002 through 2006	1/431[a]	0.232	1/3046	0.033	0.0020 (−0.0026 to 0.0066)
Hu and associates,[19] 2009	1	2002 through 2006	1/1424[a]	0.070	0/1948	0	0.0007 (−0.0007 to 0.0021)
Parolini and associates,[20] 2009	1	2003 through 2008	0/943[b]	0	1/3078	0.032	−0.0003 (−0.0010 to 0.0003)
Current study	27	2004 through 2008	8/14 838[c]	0.054	10/29 030	0.034	0.0002 (−0.0002 to 0.0006)
Pooled estimates				0.080[d]		0.030[d]	0.0005 (−0.0002 to 0.0012)
Test for homogeneity			chi-square = 18.21, df = 6, P = .0057				
Test for difference in incidence			Z = 1.59, P = .207				

CI = confidence interval; df = degrees of freedom; MIVS = microincision vitrectomy surgery; yrs = years.
[a]25-gauge system only.
[b]23-gauge system only.
[c]Two (0.030%) of 6660 eyes with the 23-gauge system; 6 (0.073%) of 8238 eyes with the 25-gauge system.
[d]Weighted incidence of postvitrectomy endophthalmitis was derived from the pooled data of 7 studies.

vitrectomy surgery were retrieved systematically from MEDLINE, Embase, and the Cochrane Library through November 2009 using the search terms endophthalmitis, incidences or rates, vitrectomy, 23-gauge, and 25-gauge. A manual search also was performed by checking the reference lists of all retrieved trials to identify studies not included in the computerized databases. Only the clinical studies that directly compared the postvitrectomy endophthalmitis rates between microincision vitrectomy surgery (23- or 25-gauge) and conventional 20-gauge vitrectomy were included. To avoid acknowledged and converted data duplication from the same group of patients, only the most recent series or largest study group was included for subsequent analysis.

• STATISTICAL ANALYSIS: For the data derived from the current survey, the incidence of acute-onset endophthalmitis associated with microincision vitrectomy surgery and conventional 20-gauge vitrectomy were compared using the chi-square test, and confidence intervals (CIs) were calculated by the percentage of binomial distribution. Other proportions also were compared using the Fisher exact test. The VA was measured using the Landolt C acuity chart and was analyzed on a logarithm of the minimal angle of resolution (logMAR) scale. Counting fingers vision was defined as 0.01 (2.0 logMAR), hand movements vision was defined as 0.005 (2.3 logMAR), light perception vision was defined as only 0.002 (2.7 logMAR), and no light perception vision was defined as 0.001 (3.0 logMAR).[28,29] Visual improvement was defined as an increase of at least 0.3 logMAR unit. Where appropriate, the Student t test and the Wilcoxon rank-sum test were used to compare the differences between groups.

After study selection and data extraction, dichotomous data from each study eligible for meta-analysis were summarized as risk differences. Considering the heterogeneity among studies, we analyzed the homogeneity statistics and then combined data using a random effects model by restricted the maximum likelihood method to achieve more conservative estimates.[30,31] The risk differences are presented with 95% CIs.

All primary analyses were performed using either JMP software version 8.0 for windows (SAS Institute, Inc, Cary, North Carolina, USA) or the meta-analyses were carried out with a commercially available software programmed by Kenichi Masui (Shinko Trading Co Ltd, Publication Department, Tokyo, Japan) with Excel. P < .05 was considered statistically significant.

RESULTS

• INCIDENCE OF POSTVITRECTOMY ENDOPHTHALMITIS IN THE CURRENT SURVEY: A total of 43 868 vitrectomies met the inclusion criteria during the study period: 29 030 cases treated with conventional 20-gauge vitrectomy, 8238 cases treated with the 25-gauge system, and 6600 cases treated with the 23-gauge system. Of these, acute-onset postvitrectomy endophthalmitis developed in 18 eyes (0.041%; 95% CI, 0.022% to 0.060%); the incidence of acute infectious endophthalmitis was 0.034% (10 cases per 29 030 eyes; 95% CI, 0.013% to 0.056%) for conventional 20-gauge PPV compared with 0.054% (8 cases per 14 838 eyes; 95% CI, 0.017% to 0.091%) for microincision vitrectomy surgery. The difference between the procedures was not significant (P = .603). Of the

TABLE 2. Preoperative Characteristics and Surgical Details of Patients with Acute-Onset Postvitrectomy Endophthalmitis

Case No.	Age (yrs)	Gender	Eye	Preoperative Diagnosis	Preoperative VA	Lens Status	Gauge for Surgery	Vitrectomy[a]	No. of Sutured Sclerotomies	Vitreous Tamponade	Surgical Time (min)	Postoperative Hypotony[b]	Systemic Medical Factors
1	69	M	R	VH, PDR	0.05	Phakic	20	Extensive	3	Fluid	72	No	Diabetes mellitus, renal dialysis
2	64	M	L	RRD	1.0	Phakic	20	Extensive	3	Silicone oil	95	No	
3	78	F	L	ERM	0.6	Phakic	20	Core	3	Fluid	45	No	
4	53	M	L	VH, PDR	0.4	Phakic	20	Extensive	3	Silicone oil	60	No	Diabetes mellitus
5	63	M	R	VH, PDR	0.1	IOL	20	Extensive	3	Fluid	90	No	Diabetes mellitus
6	59	F	R	TRD, PDR	0.5	Phakic	20	Extensive	3	Fluid	110	No	Diabetes mellitus
7	63	F	R	VH, PDR	0.1	Phakic	20	Extensive	3	Fluid	105	No	Diabetes mellitus, hypertension
8	41	M	L	TRD, PDR	0.06	Phakic	20	Extensive	3	Fluid	150	No	Diabetes mellitus
9	62	F	L	VH, BRVO	0.1	IOL	20	Extensive	3	Fluid	85	No	
10	57	M	L	Dislocated lens fragment	0.03	Aphakic	20	Core	3	Fluid	110	No	
11	70	M	L	SRH, AMD	0.1	IOL	25	Core	0	Fluid	30	Yes	
12	62	M	R	TRD, BRVO	0.2	Phakic	25	Extensive	3	Fluid	100	No	
13	66	M	R	ME, BRVO	0.2	Phakic	25	Core	0	Fluid	30	No	
14	60	M	L	ME, BRVO	0.3	Phakic	25	Extensive	0	Fluid	60	No	
15	59	F	R	DME	0.4	IOL	25	Core	0	Fluid	40	No	Diabetes mellitus
16	60	F	L	ERM	0.5	Phakic	25	Core	0	Fluid	25	No	
17	64	F	R	RRD	1.0	Phakic	23	Extensive	0	SF6	85	No	
18	65	F	L	VH, PDR	HM	IOL	23	Extensive	0	Fluid	40	No	Diabetes mellitus

AMD = age-related macular degeneration; BRVO = branch retinal vein occlusion; DME = diabetic macular edema; ERM = epiretinal membrane; F = female; HM = hand movements; IOL = intraocular lens; L = left; M = male; ME = macular edema; PDR = proliferative diabetic retinopathy; R = right; RRD = rhegmatogenous retinal detachment; SF_6 = sulfur hexafluoride; SRH = subretinal hemorrhage; TRD = traction retinal detachment; VA = visual acuity; VH = vitreous hemorrhage.

[a]Vitrectomy with peripheral vitreous shaving was defined as extensive; vitrectomy limited to the central portion without peripheral vitreous shaving was defined as a core vitrectomy.

[b]Postoperative hypotony was defined as intraocular pressure ≤ 7 mm Hg observed within 1 week after surgery.

14 838 eyes treated with microincision vitrectomy surgery, the incidence of endophthalmitis among the 25-gauge cases (6 per 8238 eyes; 0.073%) was more than twice as high as that among the 23-gauge cases (2 per 6600 eyes; 0.030%), but the difference did not reach significance (P = .451). The mean follow-up period was 25.3 ± 11.8 months (range, 6 to 60 months).

• SYSTEMATIC OVERVIEW OF DIFFERENCES IN ENDOPH-THALMITIS FREQUENCY BETWEEN MICROINCISION VIT-RECTOMY SURGERY AND CONVENTIONAL 20-GAUGE VITRECTOMY: Seven potentially relevant publications were identified in the literature search. [14–20] One study was excluded because of possible duplication of patient data from another large series.[15,16] After adding the data from the current multicenter survey, 7 retrospective studies met the criteria for subsequent meta-analysis. Because there was heterogeneity among the studies, a random-effects model (restricted maximum likelihood method) was applied for meta-analysis (Table 1). The 7 studies pooled a total of 77 956 eyes, and the pooled estimates of endoph-thalmitis after microincision vitrectomy surgery (0.080%;

95% CI, 0.030% to 0.164%) were numerically higher than that after conventional 20-gauge vitrectomy (0.030%; 95% CI, 0.012% to 0.048%); however, the difference between the groups was not significant (P = .207), with a pooled risk difference of 0.0005 (95% CI, −0.0002 to 0.0012).

• TREATMENT OUTCOMES OF POSTVITRECTOMY EN-DOPHTHALMITIS IN THE CURRENT SURVEY: The patient baseline characteristics and surgical details of the 18 eyes with postvitrectomy endophthalmitis in the current multicenter survey are shown in Table 2. All eyes were treated with topical antibiotics at the time of presentation. Of the 8 patients (5 women, 3 men) in whom acute-onset endophthalmitis developed after microincision vitrectomy surgery, 2 patients (25%) had diabetes mellitus. All surgeries were uneventful: 4 eyes with macular diseases underwent simple core vitrectomy, and 4 eyes underwent extensive vitreous removal with peripheral vitreous shaving. Seven eyes (87.5%) were left with a fluid-filled vitreous cavity at the end of surgery, whereas fluid-air exchange followed by long-acting gas tamponade was

TABLE 3. Presenting Characteristics and Treatment Results of Patients with Acute-Onset Postvitrectomy Endophthalmitis

Case No.	Days to Presentation	Presenting VA	Main Symptoms at Presentation	Clinical Findings	Organism	Intraocular Treatment	Final VA
1	5	NA	Blurred vision	Fibrin, vitreitis	Culture negative	Vitrectomy, irrigation with vancomycin, imipenem	0.1
2	1	NA	Ocular pain	Fibrin, hypopyon, retinal hemorrhages	Culture specimen not obtained	Tap with vancomycin	1.0
3	2	HM	Blurred vision	Cells, vitreitis, retinal necrosis	Culture negative	Vitrectomy, irrigation with imipenem	0.7
4	2	HM	Blurred vision	Fibrin, hypopyon	Culture negative	Vitrectomy, irrigation with imipenem	0.2
5	4	0.03	Blurred vision	Cells, fibrin, hypopyon, vitreitis, retinal vasculitis	MRSE	Vitrectomy, irrigation with vancomycin, ceftazidime, IOL extraction	0.3
6	2	NA	Ocular pain	Cells, fibrin, hypopyon, vitreitis	Culture negative	Vitrectomy, irrigation with vancomycin, ceftazidime	0.1
7	2	LP	Ocular pain	Cells, fibrin, hypopyon, vitreitis	Pneumococcus	Vitrectomy, irrigation with vancomycin, ceftazidime	HM
8	2	LP	Ocular pain	Cells, fibrin, hypopyon, vitreitis, retinal necrosis	MRSA	Vitrectomy, irrigation with vancomycin, ceftazidime	NLP
9	3	0.1	Blurred vision	Cells, fibrin, vitreitis	Culture specimen not obtained	Tap with vancomycin	0.8
10	23	HM	Blurred vision	Cells, fibrin, vitreitis	Culture negative	Vitrectomy, irrigation with vancomycin, ceftazidime	LP
11	1	HM	Ocular pain	Cells, fibrin, hypopyon, retinal hemorrhages	MRSE	Vitrectomy, irrigation with vancomycin, ceftazidime	0.1
12	3	CF	Blurred vision	Cells, fibrin, hypopyon, retinal hemorrhages	MRSE	Vitrectomy, irrigation with vancomycin, ceftazidime	1.0
13	2	NA	Blurred vision	Cells, fibrin, hypopyon, retinal hemorrhage with vasculitis	Propionibacterium acnes	Vitrectomy, irrigation with vancomycin, ceftazidime	0.9
14	2	0.03	Blurred vision	Cells, fibrin, vitreitis	Culture negative	Vitrectomy, irrigation with vancomycin, ceftazidime	0.7
15	2	0.1	Blurred vision	Cells, fibrin, vitreitis	Culture negative	Vitrectomy, irrigation with vancomycin, ceftazidime	0.6
16	2	NA	Blurred vision	Cells, fibrin, vitreitis	Culture negative	Vitrectomy, irrigation with vancomycin, ceftazidime	1.0
17	2	NA	None	Cells, fibrin, hypopyon, retinal hemorrhages	Enterococcus faecalis	Vitrectomy, irrigation with vancomycin, imipenem	0.7
18	1	HM	None	Cells, fibrin, hypopyon	MSSA	Tap with vancomycin, ceftazidime	0.1

CF = counting fingers; HM = hand movements; IOL = intraocular lens; LP = light perception; MRSA = methicillin-resistant *Staphylococcus aureus*; MRSE = methicillin-resistant *Staphylococcus epidermis*; MSSA = methicillin-sensitive *Staphylococcus aureus*; NA = data not available; NLP = no light perception; VA = visual acuity.

TABLE 4. Comparison of the Baseline Characteristics and Outcomes in Patients with Acute-Onset Postvitrectomy Endophthalmitis between Conventional 20-Gauge Surgery and Transconjunctival MIVS

Parameter	MIVS[a] (n = 8)	20-Gauge (n = 10)	P Value
Gender (female/male, no. patients)	4/4	3/7	.63
Age (yrs)			
Mean ± SD	63.3 ± 3.7	60.9 ± 9.7	.48
Range	59 to 70	41 to 78	
Indications for surgery, no. (%)			
Macular diseases	4	1	.12
Retinal detachment	2	1	
Complications related to PDR	1	6	
Others	1	2	
Preoperative VA			
Mean (range)	0.18 (HM to 1.0)	0.16 (0.03 to 1.0)	
LogMAR ± SD	0.74 ± 0.70	0.80 ± 0.52	.43
Lens status (phakic/aphakic/IOL)	5/0/3	7/1/2	.52
Vitrectomy (extensive/core)[b]	4/4	8/2	.32
Triamcinolone acetonide (used/not use)	6/2	4/6	.19
Tamponade (fluid/no fluid)[c]	6/1	8/2	1.00
Surgical time (min)			
Mean ± SD	51.3 ± 27.9	92.0 ± 29.7	.01
Range	25 to 100	45 to 150	
Days to presentation			
Mean ± SD	1.9 ± 0.6	4.6 ± 6.6	.19
Range	1 to 3	1 to 23	
Median	2	2	
Positive cultures, no. (%)	5 (63)	3 (38)[d]	.62
Treatment (vitrectomy/tap)	7/1	8/2	1.00
Final visual acuity			
Mean (range)	0.48 (0.1 to 1.0)	0.07 (NLP to 1.0)	
LogMAR ± SD	0.32 ± 0.43	1.15 ± 1.12	.03
Changes in visual acuity[e]			
LogMAR ± SD	−0.42 ± 0.46	0.35 ± 0.86	.02
≥ 0.3 logMAR unit, no. (%)	5 (63)	3 (30)	.34

F = female; logMAR = logarithm of minimal angle of resolution; M = male; MIVS = microincision vitrectomy surgery; NLP = no light perception; PDR = proliferative diabetic retinopathy; SD = standard deviation; VA = visual acuity.

[a]Includes 23- and 25-gauge microincision vitrectomy surgeries.

[b]Vitrectomy with peripheral vitreous shaving was defined as extensive; vitrectomy limited to the central portion without peripheral vitreous shaving was defined as a core vitrectomy.

[c]No fluid indicates the tamponade was silicone oil or nonexpansile long-acting gas.

[d]Culture specimens were not obtained in 2 eyes in the conventional 20-gauge vitrectomy group.

[e]Changes between preoperative and final visual acuities were evaluated using the logMAR scale.

performed in one eye (12.5%). All sclerotomies except one were self-sealing. One eye (12.5%) had postoperative hypotony (intraocular pressure, ≤ 7 mm Hg) from day 1 after surgery. Of the 10 patients (4 women, 6 men) in whom acute-onset endophthalmitis developed after conventional 20-gauge PPV, 6 patients (55%) had diabetes mellitus. All surgeries were uncomplicated; 80% of patients underwent extensive vitreous removal with peripheral vitreous shaving. Eight eyes (80%) were left with a

fluid-filled vitreous cavity at the end of surgery, whereas silicone oil tamponade was performed in 2 eyes (20%).

The presenting characteristics and treatment results of the 18 eyes are shown in Table 3. Of the 8 patients who underwent microincision vitrectomy surgery, the median time between surgery and presentation with endophthalmitis was 2 days (mean, 1.9 days; range, 1 to 3 days), and 63% of patients had blurred vision rather than ocular pain as the initial manifestation. Seven (87.5%) of the 8

eyes underwent vitrectomy with intraocular irrigation with antibiotics; the other eye underwent a tap and injection procedure with intravitreal antibiotics because of relatively mild intraocular inflammation. Vancomycin was used intravitreally in all 8 eyes, and ceftazidime was used in 7 eyes (87.5%). Culture-positive organisms were detected in 5 eyes (63%), whereas the other 3 cases were culture negative. All positive-culture organisms responded to intraocular antibiotics. The presenting VA was available for 5 eyes: hand movements (n = 2), counting fingers (n = 1), 0.1 (n = 1), and 0.03 (n = 1). After treatment, 6 eyes (75%) had a VA of 0.5 (20/40) or better and 5 eyes (63%) had visual improvement compared with that before surgery. Of the 10 patients with endophthalmitis after 20-gauge PPV, the median time between surgery and presentation with endophthalmitis was 2 days (mean, 4.6 days; range, 1 to 23 days). Eight (80%) of the 10 eyes underwent revisions with intraocular irrigation with antibiotics, and 2 eyes underwent a tap and injection procedure with intravitreal antibiotics because of relatively mild intraocular inflammation. Vancomycin was used intravitreally in 8 eyes, ceftazidime was used in 5 eyes, and imipenem was used in 2 eyes. Organisms were identified in 3 (37.5%) of the 8 eyes, and the other 5 cases were culture negative. All culture-positive organisms responded to the intraocular antibiotics. The presenting VA levels were available for 7 eyes: light perception (n = 2), hand movements (n = 3), 0.1 (n = 1), and 0.03 (n = 1). After treatment, 2 eyes (20%) had a VA of 0.5 or better, and 1 eye lost light perception. The VA improved in 3 eyes (30%) compared with that before surgery.

The baseline characteristics and treatment outcomes of the patients in whom acute-onset endophthalmitis developed were compared between groups (Table 4). Although the mean surgical times of the 8 eyes treated with microincision vitrectomy surgery were significantly shorter than in the 10 eyes treated with conventional 20-gauge vitrectomies (51.3 ± 27.9 versus 92.0 ± 29.7 minutes; P = .01), there were no significant differences in the baseline characteristics or surgical techniques used for the intraocular manipulations between groups. The times to the development of endophthalmitis were similar between groups (median, 2 days), except for 1 eye in the 20-gauge group in which endophthalmitis developed 23 days after surgery. The presenting VA generally was poor in both groups. However, the final VA and visual improvement after treatment for endophthalmitis were better in the patients who underwent microincision vitrectomy surgery.

DISCUSSION

THE CURRENT STUDY SHOWED STATISTICAL STRENGTHS over previously published reports. To the best of our knowledge, our multicenter survey is the largest population study that included 43 868 cases from 31 surgeons in 27 retina facilities and the first to survey simultaneously the postvitrectomy endophthalmitis rates for each of the 3 instrument gauges to elucidate the current trends and potential risks of postvitrectomy endophthalmitis associated with microincision vitrectomy surgery. The current survey showed that the overall incidence of acute-onset postvitrectomy endophthalmitis during the past 5 years in Japan was 0.041% (18 eyes per 43 836 cases). The incidence rate of endophthalmitis after 20-gauge vitrectomy was 0.034% (10 eyes per 29 030 cases) in the current series, which was comparable with the rates reported during the past decades (0.03% to 0.05%).[4-6] Although the acute-onset endophthalmitis rates after microincision vitrectomy surgery (including 23- and 25-gauge procedures) were higher than for the conventional 20-gauge procedure, the differences did not reach significance (0.054% vs 0.034%; P = .603). Similarly, of the 14 838 eyes treated with microincision vitrectomy surgery, a higher incidence of acute-onset postvitrectomy endophthalmitis developed in the 25-gauge group (0.073%) compared with the 23-gauge group (0.030%), but the difference did not reach significance (P = .451). The higher incidence observed in the cases treated with the 25-gauge system may be attributed partly to the 25-gauge group that included cases in which a vertical incision was created for trocar–cannula insertion during the early years after the system was introduced. The rate of acute-onset endophthalmitis after the 25-gauge system in the current series was almost equal to or slightly higher than the rates in 2 recent studies (0.070% [1 eye per 1424 cases] and 0.030% [1 eye per 3343 cases]),[17,19] but did not agree with the significantly higher incidences reported by 4 other studies (0.22% to 1.55%).[14-16,18] Therefore, we sequentially performed a systematic review and pooled data from different studies, including the current multicenter survey, and objectively reanalyzed the resultant larger data set with increased statistical power to determine more accurate incidence rates of and correct conclusions about this infrequent but devastating complication.

In the current meta-analysis, the pooled results showed no significant differences in the rates of acute-onset endophthalmitis among the procedures (P = .207; risk difference, 0.0005; 95% CI, −0.0002 to 0.0012), even though the weighted incidence rates of endophthalmitis after microincision vitrectomy surgery (0.08%) were numerically greater than after 20-gauge vitrectomy (0.03%). Similar to the theories about increased rates of endophthalmitis after cataract surgery with sutureless clear corneal incisions,[22] incomplete wound adaptation and related postoperative hypotony have received attention as high-risk factors contributing

to the development of acute-onset endophthalmitis after microincision vitrectomy surgery.[7,32,33] Recent imaging studies combined with histologic examinations have suggested a risk of bacterial contamination in the vitreous cavity and the possible mechanism of endophthalmitis associated with the transconjunctival sutureless procedure.[34,35] Therefore, several special surgical techniques have been proposed to ensure rigid self-sealing of sclerotomies and to prevent bacterial migration into the vitreous cavity through the sutureless incisions.[9,17,19,23,24,26,36] Extensive vitrectomy with intraocular irrigation to wash out the bacteria also is recommended because direct inoculation of ocular surface flora into the vitreous cavity via insertion of transconjunctival instruments may be another cause of postvitrectomy endophthalmitis.[14,17,37] These specific procedures may have substantial clinical value to minimize the potential risk of endophthalmitis after microincision vitrectomy surgery; however, these modifications may not yet have been subjected to appropriate clinical study. Given that the endophthalmitis rates after microincision vitrectomy surgery in the current multicenter survey (0.07%) were comparable with the pooled endophthalmitis rates estimated from the meta-analysis (0.08%), a simple antiseptic preparation with povidone–iodine, the only prophylactic technique that has received an intermediate clinical recommendation for preventing bacterial endophthalmitis after cataract surgery,[38] and a standard suturing technique to seal the sclerotomy if there is concern about the self-sealing properties of a transconjunctival incision, may be the best procedures for decreasing the risk of endophthalmitis after microincision vitrectomy surgery to a sporadic level, although the incidence may be slightly greater than that after conventional 20-gauge vitrectomy because of the transconjunctival approach and sutureless nature of microincision vitrectomy surgery.

In the current multicenter survey, the baseline characteristics and surgical parameters of the eyes with acute-onset postvitrectomy endophthalmitis did not differ significantly between microincision vitrectomy surgery and conventional 20-gauge vitrectomy, except that the mean surgical time was significantly shorter in the former group, as expected. Surgeons should keep in mind that acute-onset endophthalmitis may occur sporadically even after uneventful short microincision vitrectomy surgery in patients without high-risk backgrounds, as shown in the current series. Historically, visual outcomes in patients with endophthalmitis after vitrectomy generally are poor, and vision can decrease to loss of light perception in many cases.[1-3,5,6] However, the final visual outcomes in patients with endophthalmitis after microincision vitrectomy surgery in the current series were much better compared with those after conventional 20-gauge vitrectomy, despite no significant differences in the baseline characteristics and

treatment regimens for postvitrectomy endophthalmitis among the groups. The visual outcomes of acute-onset postoperative endophthalmitis generally are associated with organism virulence and the spectrum of bacterial sensitivity of the antibiotics used to treat endophthalmitis.[38] Similar to endophthalmitis after cataract surgery,[38,39] the bacterial strains isolated from specimens in eyes with endophthalmitis after microincision vitrectomy surgery in the current series were indistinguishable from the commensal organisms recovered from the eyelids, conjunctiva, or nose, which strongly suggests that the bacterial strains that cause acute-onset endophthalmitis after microincision vitrectomy surgery are associated with the ocular surface flora. All organisms isolated in the current series responded to vancomycin and ceftazidine, which may account for the better visual recovery in our series. Although commensal bacterial contamination of the ocular surface and intraocular inoculation of the flora during transconjunctival procedures may be inevitable with any prophylactic regimens,[38-40] preoperative preparation with povidone–iodine and perioperative antibiotic administration may decrease the virulent organisms on the ocular surface.[37,41] Early detection of clinically evident endophthalmitis and timely administration of appropriate antibiotics are important for acute-onset endophthalmitis after microincision vitrectomy surgery and may minimize progression of endophthalmitis and thus achieve better visual recovery.

The current study had several limitations. All studies reviewed were retrospective, and the accumulation of study populations took several years. Therefore, the quality of data obtained within a single study may be uneven. The studies in this data set are heterogeneous because of the variability in sample sizes, surgical indication criteria, surgical procedures, and perioperative aseptic protocols. Although we minimized these potential drawbacks to obtain the pooled estimates for our trend analysis using random-effects regression analysis with the weighting method, the current study failed to uncover factors critical to decreasing the risk or minimizing the severity of postvitrectomy endophthalmitis because of the study heterogeneity. Despite these limitations, by combining the results from our multicenter survey and previous studies, the current systematic review allowed us to address the recent trends in endophthalmitis after microincision vitrectomy surgery using existing data with increased statistical power.

In conclusion, the current study provided statistical strengths over previous reports that suggested that the incidence of acute-onset endophthalmitis after microincision vitrectomy surgery has decreased to a level as low as that after conventional 20-gauge vitrectomy. A better understanding of possible causes of infection and conventionally standardized antiseptic protocols combined with specific techniques or suturing to facilitate rigid

wound adaptation may account for this favorable trend in microincision vitrectomy surgery. Further studies are needed to investigate appropriate surgical procedures, that is, antiseptic protocols, specific surgical techniques, or both, to prevent acute-onset endophthalmitis after transconjunctival microincision vitrectomy surgery.

REFERENCES

1. May DR, Peyman GA. Endophthalmitis after vitrectomy. Am J Ophthalmol 1976;81(4):520–521.
2. Blankenship GW. Endophthalmitis after pars plana vitrectomy. Am J Ophthalmol 1977;84(6):815–817.
3. Ho PC, Tolentino FI. Bacterial endophthalmitis after closed vitrectomy. Arch Ophthalmol 1984;102(2):207–210.
4. Cohen SM, Flynn HW Jr, Murray TG, Smiddy WE. Endophthalmitis after pars plana vitrectomy. The Postvitrectomy Endophthalmitis Study Group. Ophthalmology 1995;102(2):705–712.
5. Aaberg TM Jr, Flynn HW Jr, Schiffman J, Newton J. Nosocomial acute-onset postoperative endophthalmitis survey. A 10-year review of incidence and outcomes. Ophthalmology 1998;105(6):1004–1010.
6. Eifrig CW, Scott IU, Flynn HW Jr, Smiddy WE, Newton J. Endophthalmitis after pars plana vitrectomy: incidence, causative organisms, and visual acuity outcomes. Am J Ophthalmol 2004;138(5):799–802.
7. Lewis H. Sutureless microincision vitrectomy surgery: unclear benefit, uncertain safety. Am J Ophthalmol 2007; 144(4):613–615.
8. Fujii GY, De Juan E Jr, Humayun MS, et al. A new 25-gauge instrument system for transconjunctival sutureless vitrectomy surgery. Ophthalmology 2002;109(10): 1807–1812.
9. Fujii GY, De Juan E Jr, Humayun MS, et al. Initial experience using the transconjunctival sutureless vitrectomy system for vitreoretinal surgery. Ophthalmology 2002;109(10): 1814–1820.
10. Taylor SR, Aylward GW. Endophthalmitis following 25-gauge vitrectomy. Eye 2005;19(11):1228–1229.
11. Taban M, Ufret-Vincenty RL, Sears JE. Endophthalmitis after 25-gauge transconjunctival sutureless vitrectomy. Retina 2006;26(7):830–831.
12. Acar N, Unver YB, Altan T, Kapran Z. Acute endophthalmitis after 25-gauge sutureless vitrectomy. Int Ophthalmol 2007;27(6):361–363.
13. Matsuyama K, Kunitomi K, Taomoto M, Nishimura T. Early-onset endophthalmitis caused by methicillin-resistant Staphylococcus epidermidis after 25-gauge transconjunctival sutureless vitrectomy. Jpn J Ophthalmol 2008;52(6):508–510.
14. Kunimoto DY, Kaiser RS. Incidence of endophthalmitis after 20- and 25-gauge vitrectomy. Ophthalmology 2007;114(12): 2133–2137.
15. Shaikh S, Ho S, Richmond PP, Olson JC, Barnes CD. Untoward outcomes in 25-gauge versus 20-gauge vitreoretinal surgery. Retina 2007;27(8):1048–1053.
16. Scott IU, Flynn HW Jr, Dev S, et al. Endophthalmitis after 25-gauge and 20-gauge pars plana vitrectomy: incidence and outcomes. Retina 2008;28(1):138–142.
17. Shimada H, Nakashizuka H, Hattori T, Mori R, Mizutani Y, Yuzawa M. Incidence of endophthalmitis after 20- and 25-gauge vitrectomy causes and prevention. Ophthalmology 2008;115(12):2215–2220.
18. Chen JK, Khurana RN, Nguyen QD, Do DV. The incidence of endophthalmitis following transconjunctival sutureless 25- vs 20-gauge vitrectomy. Eye 2009;23(4):780–784.
19. Hu AY, Bourges JL, Shah SP, et al. Endophthalmitis after pars plana vitrectomy a 20- and 25-gauge comparison. Ophthalmology 2009;116(7):1360–1365.
20. Parolini B, Romanelli F, Prigione G, Pertile G. Incidence of endophthalmitis in a large series of 23-gauge and 20-gauge transconjunctival pars plana vitrectomy. Graefes Arch Clin Exp Ophthalmol 2009;247(7):895–898.
21. Martidis A, Chang TS. Sutureless 25-gauge vitrectomy: risky or rewarding? Ophthalmology 2007;114(12):2131–2132.
22. Taban M, Behrens A, Newcomb RL, et al. Acute endophthalmitis following cataract surgery: a systematic review of the literature. Arch Ophthalmol 2005;123(5):613–620.
23. Shimada H, Nakashizuka H, Mori R, Mizutani Y, Hattori T. 25-gauge scleral tunnel transconjunctival vitrectomy. Am J Ophthalmol 2006;142(5):871–873.
24. Rizzo S, Genovesi-Ebert F, Vento A, Miniaci S, Cresti F, Palla M. Modified incision in 25-gauge vitrectomy in the creation of a tunneled airtight sclerotomy: an ultrabiomicroscopic study. Graefes Arch Clin Exp Ophthalmol 2007; 245(9):1281–1288.
25. Eckardt C. Transconjunctival sutureless 23-gauge vitrectomy. Retina 2005;25(2):208–211.
26. Shimada H, Nakashizuka H, Hattori T, Mori R, Mizutani Y, Yuzawa M. Conjunctival displacement to the corneal side for oblique-parallel insertion in 25-gauge vitrectomy. Eur J Ophthalmol 2008;18(5):848–851.
27. Results of the Endophthalmitis Vitrectomy Study. A randomized trial of immediate vitrectomy and of intravenous antibiotics for the treatment of postoperative bacterial endophthalmitis. Endophthalmitis Vitrectomy Study Group. Arch Ophthalmol 1995;113(12):1479–1496.

28. Holladay JT. Proper method for calculating average visual acuity. J Refract Surg 1997;13(4):388–391.

29. Schulze-Bonsel K, Feltgen N, Burau H, Hansen L, Bach M. Visual acuities "hand motion" and "counting fingers" can be quantified with the Freiburg visual acuity test. Invest Ophthalmol Vis Sci 2006;47(3):1236–1240.

30. Berkey CS, Hoaglin DC, Mosteller F, Colditz GA. A random-effects regression model for meta-analysis. Stat Med 1995;14(4):395–411.

31. Berkey CS, Hoaglin DC, Antczak-Bouckoms A, Mosteller F, Colditz GA. Meta-analysis of multiple outcomes by regression with random effects. Stat Med 1998;17(22):2537–2550.

32. Acar N, Kapran Z, Unver YB, Altan T, Ozdogan S. Early postoperative hypotony after 25-gauge sutureless vitrectomy with straight incisions. Retina 2008;28(4):245–252.

33. Hsu J, Chen E, Gupta O, Fineman MS, Garg SJ, Regillo CD. Hypotony after 25-gauge vitrectomy using oblique versus direct cannula insertions in fluid-filled eyes. Retina 2008; 28(7):937–940.

34. Singh A, Chen JA, Stewart JM. Ocular surface fluid contamination of sutureless 25-gauge vitrectomy incisions. Retina 2008(4);28:553–557.

35. Taban M, Ventura AA, Sharma S, Kaiser PK. Dynamic evaluation of sutureless vitrectomy wounds: an optical coherence tomography and histopathology study. Ophthalmology 2008;115(12):2221–2228.

36. Gupta OP, Weichel ED, Regillo CD, et al. Postoperative complications associated with 25-gauge pars plana vitrectomy. Ophthalmic Surg Lasers Imaging 2007;38(4):270–275.

37. Tominaga A, Oshima Y, Wakabayashi T, Sakaguchi H, Hori Y, Maeda N. Bacterial contamination of the vitreous cavity associated with transconjunctival 25-gauge microincision vitrectomy surgery. Ophthalmology 2010;117(4):811–817.

38. Ciulla TA, Starr MB, Masket S. Bacterial endophthalmitis prophylaxis for cataract surgery: an evidence-based update. Ophthalmology 2002;109(1):13–24.

39. Inoue Y, Usui M, Ohashi Y, Shiota H, Yamazaki T; Preoperative Disinfection Study Group. Preoperative disinfection of the conjunctival sac with antibiotics and iodine compounds: a prospective randomized multicenter study. Jpn J Ophthalmol 2008;52(3):151–161.

40. Speaker MG, Milch FA, Shah MK, Eisner W, Kreiswirth BN. Role of external bacterial flora in the pathogenesis of acute postoperative endophthalmitis. Ophthalmology 1991; 98(5):639–649.

41. Binder C, de Kaspar HM, Engelbert M, Klauss V, Kampik A. Bacterial colonization of conjunctiva with Propionibacterium acnes before and after polyvidone iodine administration before intraocular interventions. Ophthalmologe 1998;95(6):438–441.

APPENDIX

● THE JAPAN MICROINCISION VITRECTOMY SURGERY STUDY GROUP: Y. Oshima (P.I.), S. Kusaka, Department of Ophthalmology, Osaka University Medical School, Suita; M. Ohji, H. Kawamura, Department of Ophthalmology, Shiga University of Medical Science, Otsu; F. Shiraga, H. Yamaji (P.I.), Department of Ophthalmology, Kagawa University Faculty of Medicine, Takamatsu; S. Ataka, Department of Ophthalmology, Osaka City University Graduate School of Medicine, Osaka; H. Enaida, Department of Ophthalmology, National Hospital Organization Kyushu Medical Center, Fukuoka; M. Hashida, Department of Ophthalmology, Machida Hospital, Kochi; M. Inoue (P.I.), Department of Ophthalmology, Kyorin Eye Center, Mitaka; R. Ideta, Y. Inoue, Department of Ophthalmology, School of Medicine, The University of Tokyo, Tokyo; M. Ishida, Department of Ophthalmology, National Defense Medical College, Tokorozawa; K. Kadonosono (P.I.), Department of Ophthalmology, Yokohama City University Medical Center, Yokohama; J. Kiryu, Department of Ophthalmology, Kawasaki Medical School, Kurashiki; H. Kimura (P.I.), Nagata Eye Clinic, Nara; A. Kobori, Department of Ophthalmology, Fukui Red Cross Hospital, Fukui; H. Kunikata, Department of Ophthalmology, Tohoku University School of Medicine, Sendai; T. Kurachi, Department of Ophthalmology, Takayama Red Cross Hospital, Takayama; T. Kurakazu, Department of Ophthalmology, Hidaka Medical Center, Toyooka Hospital, Toyooka; A. Nishimura, Department of Ophthalmology, Kanazawa University Graduate School of Medicine, Kanazawa; T. Okanouchi, Department of Ophthalmology, Kurashiki Medical Center, Kurashiki; S. Osawa, Department of Ophthalmology, Okanami General Hospital, Iga; T. Sakuraba, Department of Ophthalmology, Aomori Prefectural Central Hospital, Aomori; T. Sato, Department of Ophthalmology, Gunma University School of Medicine, Maebashi; H. Shinoda, Department of Ophthalmology, School of Medicine, Keio University, Tokyo; K. Suzuma, Department of Ophthalmology, Shizuoka General Hospital, Shizuoka; M. Taomoto, Department of Ophthalmology, Kansai Medical University Hirakata Hospital, Hirakata; Y. Tsukahara, Department of Ophthalmology, Kobe University Graduate School of Medicine, Kobe; N. Chikamoto, Department of Ophthalmology, Yamaguchi University Graduate School of Medicine, Yamaguchi; and M. Yoshida (P.I.), Department of Ophthalmology, Nagoya City University Graduate School of Medical Sciences, Nagoya.

P.I. = principal investigator.

Biosketch

Yusuke Oshima has completed his education and is currently an associate professor at Osaka University Medical School in Japan. He has expertise in vitreoretinal disease and surgery. Dr. Oshima has published many articles in professional journals, presented at a large number of international congresses, and conducted many international invitational lectures and surgical demonstrations throughout Asia and Europe. His research is focused on developing new technologies for vitreoretinal surgery.

Wavefront analysis and ultrastructural findings in an eye with posterior lentiglobus

Yoko Murakami, MD,[a] Shunji Kusaka, MD,[a] Nobutsugu Hayashi, MD,[b] Kaori Soga, MD,[a] and Takashi Fujikado, MD[a]

An 8-year-old girl with unilateral posterior lenticoglobus underwent lens aspiration and intraocular lens implantation. Wavefront analysis performed before surgery to assess the surgical indication showed a higher-order aberration of 0.502 μm root mean square. After surgery, the value decreased to 0.132 μm root mean square. Preoperative best-corrected visual acuity of 0.1 improved to 0.3 postoperatively. Electron-microscopic examinations of the posterior capsule revealed unusual nodular structures and variations in capsular density.

P osterior lentiglobus is a rare disease characterized by unilateral or bilateral conical or hemispherical protrusion of the posterior lens surface with or without central posterior subcapsular lens opacity.[1] In most cases, this disorder is unilateral, sporadic, and occurs at younger ages. The patients' visual acuity gradually decreases as the result of progressive protrusion of the lens, leading to increased irregular astigmatism, lens opacity (Figure 1), or both.[1] We report a case of unilateral posterior lentiglobus that was treated by lens aspiration and intraocular lens implantation. Before and after surgery, wavefront analysis was performed. Histopathologic examinations of the posterior capsule also were conducted.

Case Report

An 8-year-old girl was referred to Osaka University Hospital, Osaka, Japan, for evaluation of decreased visual acuity in the right eye. The patient's best-corrected Snellen-equivalent visual acuity at the first visit was 0.1 (−1.5 −6.0 ×20) in the right eye and 1.5 (+0.50) in the left eye. Slit-lamp examination showed protrusion of the posterior lens surface (Figure 1A) with a subcapsular star-shaped opacity in the right eye. No other abnormal findings were detected in either eye. The parents reported no family history of any ocular disorders.

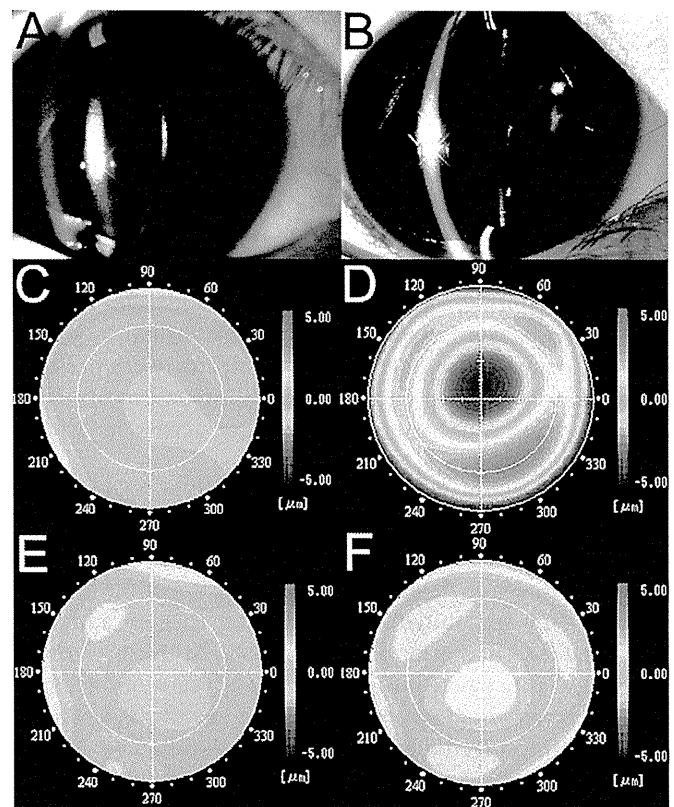Wavefront aberrometry with Topcon KR-9000PW (Topcon Corporation, Tokyo, Japan) showed −7.0 D of

FIG 1. Clinical images and wavefront aberrometry from the right eye of an 8-year-old girl with posterior lentiglobus. A, Preoperative slit-lamp image. B, postoperative image showing that the IOL is securely fixated in the bag with a posterior capsule opening. Wavefront aberrometry demonstrates the extent of higer-order aberrations preoperatively in the cornea (C) and eye (D). Postoperatively, the appearance is unchanged in the cornea (E) but improved in the eye (F).

astigmatism in the right eye and 0.502 and 0.134 μm root mean square (RMS) ocular total high-order aberrations (HOAs) with a 4-mm diameter pupil in the right and left eyes, respectively. The map of ocular HOAs showed a slower wavefront in the center corresponding to that part of the circular cone and a faster wavefront in the periphery in a circular manner (Figure 1).[2] Yet, the map of corneal HOAs was homogeneous, suggesting that the ocular HOAs originated from the lens.

Lens aspiration and intraocular lens (IOL) implantation were performed to correct the irregular astigmatism. After creation of an anterior continuous curvilinear capsulorhexis and lens aspiration, the anterior chamber and the capsular bag were filled with 1% sodium hyaluronate (Opegan Hi;

Santen Pharmaceutical Co, Ltd, Osaka, Japan). A posterior continuous curvilinear capsulorhexis 5 mm in diameter was created, followed by anterior vitrectomy. The IOL was fixated by the use of an optic capture technique, that is, the haptics of a 3-piece acrylic IOL were inserted in the capsular bag and the optics was displaced behind the posterior capsule.[3]

A capsulorhexis fragment obtained from the posterior continuous curvilinear capsulorhexis at the time of surgery was fixed in 2.5% glutaraldehyde. It was dehydrated in increasing concentrations of ethanol and embedded in Epon 812 (TAAB Laboratories Equipment Ltd, Aldermaston, UK). Ultrathin sections for electron microscopy were stained with uranyl acetate and citrate. Specimens were observed by a transmission electron microscope. The lens capsular thickness varied from 2.3 μm to 8.4 μm, with the thinnest diameter in the center and the thickest at the periphery of the specimen. A small amount of lens cortex was present on the capsular surface, but no nuclei of lens epithelial cells were present. A few unusual small nodules with the same electron density as the capsule were present on the capsular surface. In some areas, the posterior capsule exhibited variations in electron density across its width (Figure 2).

One week postoperatively, the patient's visual acuity was 0.2 (+3.0 −3.0 × 5) in the right eye. Wavefront aberrometry showed −3.7 D of astigmatism, 0.132 μm RMS ocular total HOAs, and a 4-mm diameter pupil. Occlusion of the left eye 3 hours daily was initiated 1 week after surgery and was continued for 18 months postoperatively. At the 18-month follow-up visit, when the patient was 9 years of age, her best-corrected visual acuity in the right eye was 0.3, which remained unchanged during the 48-month follow up.

Discussion

Cataract surgery should be considered carefully in young patients on account of postoperative loss of accommodation. In patients with lentiglobus with no or mild lens opacity, it is sometimes difficult to judge whether cataract surgery would be beneficial. Wavefront analysis may be helpful in these cases because it can precisely differentiate lenticular HOAs from corneal aberrations and can quantitate the HOAs.[4]

In our patient, the preoperative HOAs was 0.502 μm RMS in the right eye, which was much greater than in the left eye (0.134 μm RMS). A variation exists in the RMS value in normal subjects,[5] and a HOA of 0.15 μm RMS or less is accepted as normal with a 4-mm pupil.

The ocular total HOAs and quasispherical aberrations significantly improved postoperatively in our patient. The reason for the limited improvement in the best-corrected visual acuity after occlusion treatment may be that the patient was already beyond the age limit for amblyopia treatment. We did not find discontinuous portions or disruptions in the posterior lens capsule, as has been described previously.[6-8]
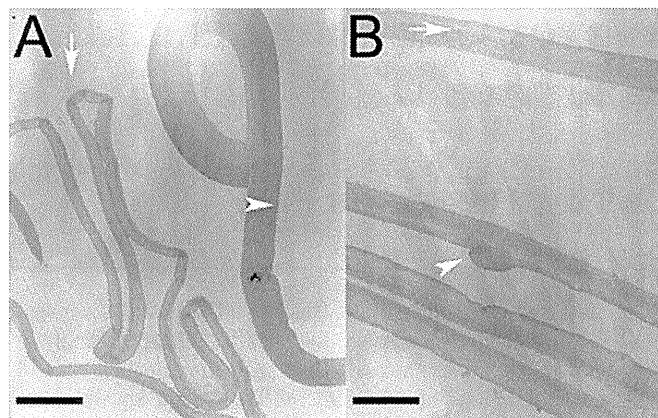

FIG 2. Transmission electron microscopy of the posterior lens capsule. A, The central capsule is on the left and the peripheral capsule is on the right. There is a marked difference in the thicknesses. The thinnest diameter is approximately 2.3 μm (arrow). The arrowhead indicates the edge of the posterior continuous curvilinear capsulorhexis (bar = 6.67 μm). B, A nodular structure on the lens capsule (arrowhead) and variations in capsule (arrow) electron density (bar = 5 μm).

To our knowledge, the unusual nodular structures and variations in electron density of the posterior lens capsule have not been reported previously in posterior lentiglobus; they could represent pathological changes of the posterior lens capsule in the current case.

Literature Search

PubMed was searched, on August 4, 2009, for the following terms: *nodule*, *nodular structure*, *lens capsule*, and *posterior lenticonus*.

References

1. Amaya L, Taylor D, Russell-Eggitt I, Nischal KK, Lengyel D. The morphology and natural history of childhood cataracts. Surv Ophthalmol 2003;48:125-44.
2. Mrochen M. Retinal imaging aberrometry: Principles and application of Tscherning aberrometer. In: Krueger RR, Applegate RA, MacRae SM, editors. Wavefront customized visual correction. Thorofare, NJ: Slack Inc.; 2004. 137-43.
3. Gimbel HV, DeBroff BM. Posterior capsulorhexis with optic capture: Maintaining a clear visual axis after pediatric cataract surgery. J Cataract Refract Surg 1994;20:658-64.
4. Ninomiya S, Maeda N, Kuroda T, Saito T, Fujikado T, Tano Y. Evaluation of lenticular irregular astigmatism using wavefront analysis in patients with lenticonus. Arch Ophthalmol 2002;120:1388-93.
5. Fujikado T, Kuroda T, Ninomiya S, et al. Age-related changes in ocular and corneal aberrations. Am J Ophthalmol 2004;138:143-6.
6. Junk AK, Stefani FH, Ludwig K. Bilateral anterior lenticonus: Scheimpflug imaging system documentation and ultrastructural confirmation of Alport syndrome in the lens capsule. Arch Ophthalmol 2000; 118:895-7.
7. Makley TA Jr. Posterior lenticonus; Report of a case with histologic findings. Am J Ophthalmol 1955;39:308-12.
8. Kato T, Watanabe Y, Nakayasu K, Kanai A, Yajima Y. The ultrastructure of the lens capsule abnormalities in Alport's syndrome. Jpn J Ophthalmol 1998;42:401-5.

Efficacy of Suprachoroidal–Transretinal Stimulation in a Rabbit Model of Retinal Degeneration

Kentaro Nishida,[1] Motohiro Kamei,[1] Mineo Kondo,[2] Hirokazu Sakaguchi,[1] Mihoko Suzuki,[1] Takashi Fujikado,[1] and Yasuo Tano[1]

PURPOSE. To develop a middle-sized animal model of outer retinal degeneration and to evaluate the effectiveness of suprachoroidal–transretinal stimulation (STS) in eliciting cortical potentials from this model.

METHODS. Twelve rabbits were intravenously injected with 0.47 mg/kg verteporfin and the retinas were irradiated with a red light for 90 minutes. Fluorescein angiography and full-field and focal electroretinography (ERG) were performed at 7 and 28 days after the irradiation. Electrically evoked potentials (EEPs) were elicited by electrical stimulation, with the STS electrode implanted over the irradiated region, 1 month and 1 year after the irradiation. EEPs were also recorded from three rabbits before and after retinotomy of the normal retina surrounding the degenerated area, to eliminate the influence of stray currents. The retina beneath the site of the STS electrode was examined histologically at 1 month (group 1) and 1 year (group 2) after the irradiation.

RESULTS. An extensive area of degeneration was detected histologically, mainly in the outer retina after the irradiation. Focal ERGs were not recorded when the stimulus was confined to the irradiated area; however, EEPs were successfully elicited by STS of the same area 1 month and 1 year after the irradiation. The 360° retinectomy did not significantly alter the amplitudes, the implicit times, or the thresholds of EEPs evoked by STS.

CONCLUSIONS. Verteporfin with light irradiation induces degeneration predominantly in the outer retinal layers in rabbits. The elicitation of EEPs by STS from the degenerated area suggests that the STS system may be useful in patients with retinitis pigmentosa. (*Invest Ophthalmol Vis Sci.* 2010;51:2263–2268) DOI:10.1167/iovs.09-4120

Despite extensive attempts by genetic manipulation and artificial prosthetic devices, a practical solution for the visual decrease in patients with retinitis pigmentosa (RP) has not been obtained. Because some of the inner retinal neurons are somewhat preserved in RP patients,[1,2] several research groups are investigating whether an intraocular retinal prosthesis can restore vision in these patients by activating the functioning neurons.[3-7]

We have developed a new method of stimulating the retina called suprachoroidal–transretinal stimulation (STS),[8] and ex-

periments on normal rabbits[9,10] and RCS rats[11] have shown that electrically evoked potentials (EEPs) can be elicited by stimulating the retina by STS. However, a middle-sized animal model with damage predominantly in the outer retinal layer, as is observed in eyes of RP patients, is needed to evaluate the effectiveness of the STS system more completely. RCS rats, S334ter rats, and P23H rats are established animal models Steinberg RH, et al. *IOVS* 1996;37:ARVO Abstract 3190)[12,13] of degeneration of the outer retinal layers, including the photoreceptors. Unfortunately, a rat eye is relatively small, which makes it difficult to implant an STS system that might be used in humans. A larger size eye model is necessary, because a safe and effective current level has not been determined in eyes of a size comparable to that of humans.

Several dog models of retinal degeneration have been identified,[14-16] but investigating a group of dogs is difficult because of the cost and labor. Thus, the purpose of this study was to develop a middle-sized animal model with predominant degeneration of the outer retinal layer which is easily available, not expensive, and easy to handle. We selected the commonly used laboratory rabbit, and induced degeneration of the outer retinal layers including the photoreceptors by photochemical damage with verteporfin. We then evaluated the efficacy of the STS system in this model.

MATERIALS AND METHODS

Animals

Twelve eyes of 12 Dutch-belted rabbits (weighing 2.0–2.3 kg; Biotech, Saga, Japan) were used. All procedures conformed to the ARVO Statement for the Use of Animals in Ophthalmic and Vision Research. Every effort was made to minimize animal discomfort and to limit the number of animals to that necessary to obtain statistical significance. Nine rabbits were used for developing the retinal degeneration and the functional evaluation of the STS system; five rabbits (group 1) were used for the evaluation at 1 month, and four rabbits (group 2) were used for the evaluation at 1 year. An additional three rabbits (group 3) were used to test the validity of the model.

Light Irradiation with Verteporfin

Rabbits were anesthetized with an intramuscular injection of ketamine (33 mg/kg) and xylazine (8.5 mg/kg), and the pupils were dilated with 0.5% tropicamide and 0.5% phenylephrine hydrochloride. Verteporfin (Visudyne; Novartis, Basel, Switzerland) was injected through an ear vein at a dose of 0.47 mg/kg. This dose was determined from the results of a study of photodynamic therapy (PDT) in monkeys[17] and the results of our pilot study with 0.24, 0.47, and 0.96 mg/kg of verteporfin in rabbits. Verteporfin was reconstituted as recommended by the manufacturer.

Light irradiation was applied 5 minutes after the verteporfin infusion. A red light-emitting diode (LED; MCEP-CR8; Moritex, Tokyo, Japan) with peak emission at 630 nm was placed next to the surface of the diffuser contact lens (illuminance was 8.0×10^4 lux). The retina was irradiated from three directions—the center, nasal, and temporal

to the visual streak—with an irradiation duration of 30 minutes in each direction, which resulted in a total irradiation time of 90 minutes.

Fundus Photography and Fluorescein Angiography

Fundus photography and FA were performed with a fundus camera (TRC-50IX; Topcon, Tokyo, Japan), with the animals under general anesthesia before and at 1 month (group 1) and 1 year (group 2) after the irradiation with verteporfin. For FA, 0.075 mL/kg of 10% sodium fluorescein was injected intravenously.

Full-Field ERGs

Dark-adapted, full-field ERGs were recorded in all group 1 rabbits, 1 month after the light exposure. After 20 minutes of dark adaptation and pupil dilation, the rabbits were anesthetized with an intramuscular injection of ketamine (40 mg/kg) and xylazine (4 mg/kg), and the ERGs were picked up with a corneal Burian-Allen bipolar electrode (Hansen Ophthalmic Development Laboratories, Iowa City, IA). The rabbits were placed in a Ganzfeld bowl and stimulated with stroboscopic stimuli of 1.7 log cd-s/m^2 (photopic units). Ten responses were averaged with a stimulus interval of 10 seconds. The a-wave amplitude was measured from the baseline to the first negative trough, the b-wave from the negative trough to the positive peak.

Focal ERGs

Focal ERGs were recorded from all group 1 rabbits, 1 week and 1 month after irradiation. The techniques used for eliciting and recording focal ERGs have been described in detail.[18,19] Briefly, focal ERGs were elicited by placing the stimulus spot on the visual streak. The position of the spot on the fundus was monitored during the recording with a modified infrared fundus camera. The same Burian-Allen bipolar contact lens electrode was used to record the focal ERGs. The luminances of the stimulus and the background were 30.0 and 3.0 cd/m^2, respectively. A 5- or 30-Hz rectangular stimulus (50% on and 50% off) was used, and a 15° stimulus spot was placed on the visual streak. A total of 512 responses were averaged by a signal processor, and the time constant was 0.03 second with a 300-Hz high-cut filter.

Electrical Stimulation and Recording of EEPs at the Visual Cortex

Cortical Electrodes. With the animal under deep general anesthesia, the top of the skull was exposed and 1-mm holes were drilled through the skull 8 mm anterior to the lambdoid suture and 7 mm to the right and left of the midline. Then, screw-type stainless steel recording electrodes coated with silver, were screwed into the skull to make electrical contact with the dura mater. The reference electrode was then screwed into the skull at the bregma.

Stimulating Electrode. A single stimulating electrode was used. The wire (90% platinum, 10% iridium; diameter, 60 μm) was insulated with silicon and embedded in a 2-mm horizontal × 5.5-mm vertical × 0.1-mm-thick parylene plate. The tip of the wire was connected to a 500-μm-diameter single stimulating platinum electrode (see Fig. 3A). The inferior surface of the sclera was exposed by cutting the inferior rectus and the inferior oblique muscles. A scleral pocket (3 × 5 mm) was created just over the irradiated area on the visual streak. The electrode plate was then implanted into the scleral pocket and sutured with 5-0 Dacron onto the sclera just above the pocket. The insulated strand lead from the electrode was sutured at the limbus with 5-0 Dacron. The implanted electrode was confirmed to be located just under the damaged area of the visual streak by binocular ophthalmoscopy.

An electronic stimulator (SEN-7203; Nihon Kohden, Shinjyuku, Japan) was connected through a stimulus isolation unit (A-395R; World Precision Instruments, Sarasota, FL) to the STS electrode. The reference electrode was a platinum wire coated with polyurethane resin, and approximately 3 mm of the tip was exposed. The wire was inserted into the vitreous cavity and was fixed 1 mm posterior to the limbus with 8-0 Vicryl.

Eliciting EEPs

EEPs were recorded 1 month (groups 1 and 3) and 1 year (group 2) after irradiation. The electrical stimulating current was change from 50 to 1000 μA, and biphasic pulses were used for the electrical stimulation. The biphasic pulses consisted of current flowing from the vitreal electrode to the STS electrode in one phase and with current flowing from the STS electrode to the vitreal electrode. The duration of both phases was 0.5 ms. The threshold current for eliciting an EEP was determined by decreasing the electric current in steps. The minimum electric current that elicited the first or second positive peak of the EEP (P1 or P2) was defined as the threshold current. The EEP amplitude was measured from the baseline to the first positive trough.

Assessing Validity of This Model

To investigate the influence of stray current beyond the degenerative area where the STS stimulating electrode was placed, we removed 360° of the normal retina surrounding the degenerated area by vitrectomy and retinectomy. EEPs were recorded from the degenerated retina immediately after the retinectomy by stimulating with the STS electrode in three irradiated eyes (group 3; Figs. 3C1, 3C2). Then, EEPs were recorded before and again immediately after retinectomy in those eyes that had only the degenerated retina and optic nerve.

Histologic Study

Histologic studies were performed in the areas where the electrode was placed 1 month (group 1) and 1 year (group 2) after, to ensure that the outer retina was degenerated. After the EEPs were recorded, the stimulating electrode was removed from the eye, and the rabbits were euthanatized with a 5-mL intravenous injection of pentobarbital (50 mg/mL). The eyes were enucleated, fixed with 4% paraformaldehyde, dissected, and embedded in optimal cutting temperature compound (Tissue-Tek; Sakura Finetechnical Co. Ltd. Tokyo, Japan). Cryosections of 7-μm thickness were cut and stained with hematoxylin and eosin. The sections were examined under a light microscope and photographed with a CCD camera (AxioCam; Carl Zeiss Japan, Tokyo, Japan). The images were then analyzed (AxioVision 2.0 software for Windows; Carl Zeiss Japan). The numbers of nuclei in the outer nuclear layer (ONL), inner nuclear layer (INL), and ganglion cell layer (GCL) were counted at ×40 magnification in all eyes from groups 1 and 2. Three sections from each eye were counted; at the center of the stimulating electrode, and at ±500 μm away from the electrode. Sections were oriented along the visual streak.

Statistical Analyses

The Mann-Whitney test was used to calculate the significance of the differences in the full-field ERGs, EEPs, and cell counts between control and irradiated eyes. Paired t-tests were used to calculate the significance of the differences in the EEPs before and after retinectomy in group 3. $P < 0.05$ was considered statistically significant (all analyses: SigmaStat, ver.2.0; Systat, San Jose, CA).

RESULTS

Retinal Degeneration Model

A well-defined chorioretinal atrophy was observed in all eyes by indirect ophthalmoscopy at 1 month after the irradiation. In addition, a hypofluorescent area, that corresponded to the area of the chorioretinal atrophy was seen by FA. The lesion and the hypofluorescent area remained unchanged for 1 year, whereas the area of occluded choriocapillaris increased (Figs. 1A–F).

Histologic Examination of the Retina beneath the Electrode

Photoreceptors and nuclei in the ONL were almost completely absent beneath the area where the electrode array was placed. The relative number of cells (experimental eye/control eye)
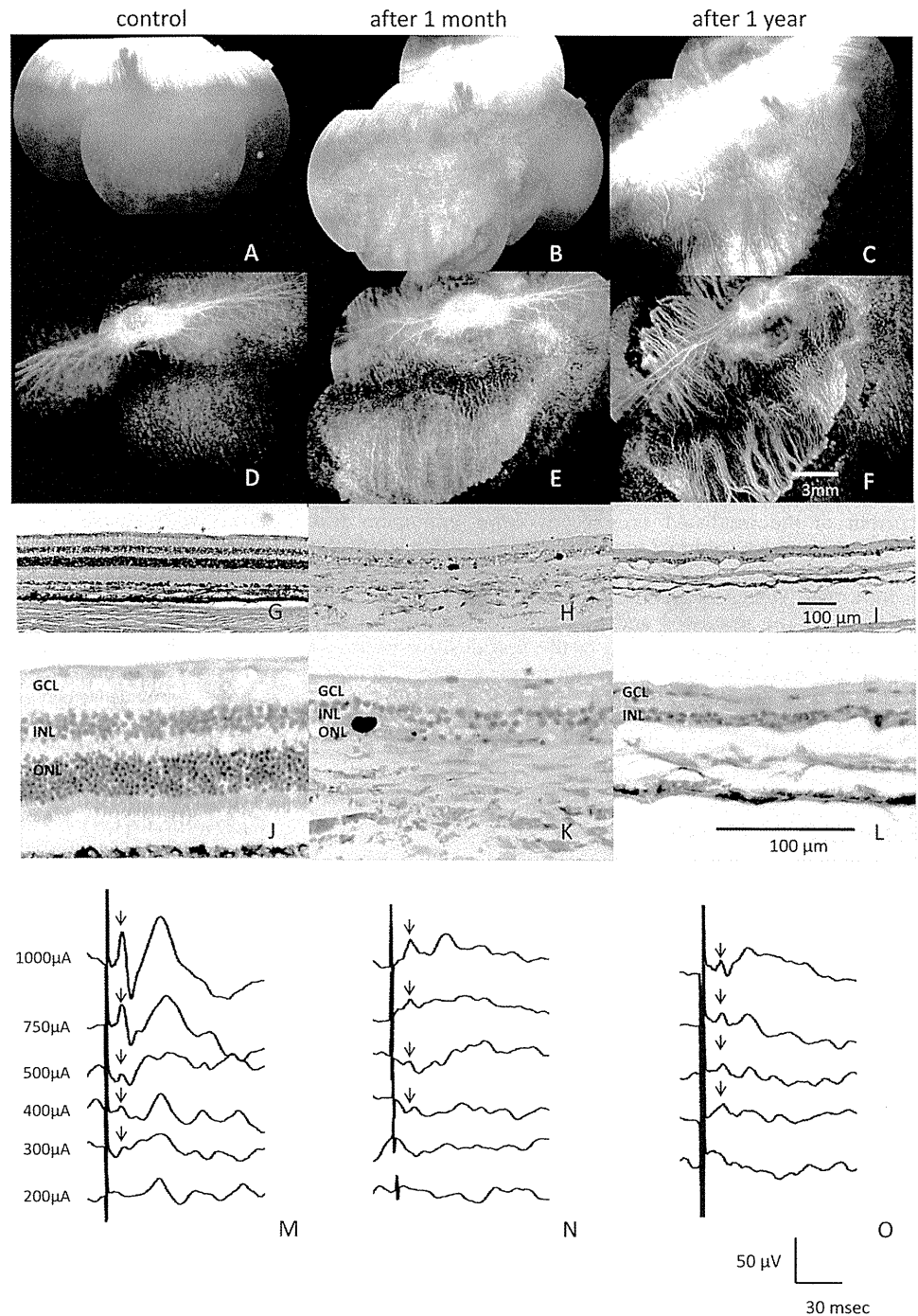
FIGURE 1. Representative fundus photographs (A-C), fluorescein angiograms (D-F), photomicrographs of the area where the electrode was placed (G-L), and EEPs (M-O) of the control and irradiated eyes at 1 month and 1 year after the irradiation with a red LED after intravenous verteporfin. (B, C, E, F) Atrophy of RPE and choriocapillaris can be seen. The occlusion of the choriocapillaris continued to be present at 1 year (F). Histopathology of the control eye (G, J) showed that the ONL and outer layers were fibrotic (H, I, K, L). At 1 year, the atrophy of the choroid had progressed, and the number of cells in the INL had decreased but the GCL was preserved (I, L). Scale, 100 μm. The EEPs (*arrows*) recorded after biphasic electrical pulses from the STS electrodes implanted in the control eye and degenerated eyes at 1 month and 1 year after irradiation.

was reduced to 1.5% ($P = 0.003$) in the ONL, to 56.8% ($P = 0.006$) in the INL, and to 84.5% ($P = 0.317$) in the GCL (Figs. 1G-L; Table 1). At 1 year after irradiation, the cell counts in the INL were reduced to 66% ($P = 0.004$) of the control, but those in the GCL were not significantly reduced ($P = 0.903$).

Full-Field and Focal ERGs

Representative waveforms of the dark-adapted, full-field ERGs are shown in Figure 2A, and the means ± SDs of the amplitude and implicit times of the a- and b-waves are shown in Figure 2B. We found that the amplitudes of both the a- and b-waves were reduced to about one half of the control ERGs ($P < 0.05$) at 1 month after irradiation (group 1). There was no significant difference in the implicit times of the a- and b-waves before and after the irradiation ($P = 0.548$ and $P = 0.095$).

We then recorded focal ERGs to examine the retinal function in the irradiated area. We could not record any responses with the stimulus spot placed on the irradiated area from all the eyes. The amplitudes of focal ERGs were less than the noise level (0.3 μV) for all rabbits (Fig. 2C), whereas focal ERGs with both 5- and 30-Hz stimuli from all the control eyes were recorded.

Evaluation of STS

EEPs were successfully elicited by STS from all eyes in all groups (Figs. 1M-O, 3D, 3E). The mean threshold current evoking the EEP in the irradiated eyes at 1 month after irradiation was 431.3 ± 143.8 μA and that of the control eyes was 360.0 ± 114.0 μA. This difference was not significant ($P = 0.262$). The average current density was 20.5 and 16.4 μC/cm²

TABLE 1. Cell Counts in the Control and Irradiated Eyes

	ONL	INL	GCL
Control	475.8 ± 84.9	186.0 ± 31.2	14.8 ± 3.9
1 Month after			
irradiation	7.0 ± 10.3	105.6 ± 31.1	12.5 ± 3.8
P^*	**0.003**	**0.006**	0.317
1 Year after			
irradiation	0	69.3 ± 32.4	14.4 ± 3.3
P^*	**0.004**	**0.004**	0.903

Data are expressed as the mean ± SD.

* Mann-Whitney Rank Sum Test with significant differences in bold.

for the irradiated and control eyes, respectively ($P = 0.262$). The implicit times of the first positive waves of the EEPs in the irradiated eyes and in the control eyes were 13.4 ± 8.7 and 17.1 ± 12.4 ms, respectively ($P = 0.662$). The mean threshold current of the irradiated eyes 1 year after irradiation was 300.0 ± 141.4 μA (group 2) and was 233.3 ± 115.5 μA in the control eyes. None of these differences was significant ($P = 0.400$). The averaged electrical density was 13.6 and 10.6 μC/cm^2 for the irradiated and the control eyes, respectively ($P = 0.400$). The implicit times of the first positive waves of the EEPs in irradiated eyes and in control eyes were 17.9 ± 4.7 and 13.9 ± 5.9 ms ($P = 0.229$).

There was no significant difference in the threshold current of the irradiated eyes at 1 month (431.3 ± 143.8 μA) and 1 year (300.0 ± 141.4 μA) after the irradiation ($P = 0.413$).

Influence of Stray Current

The threshold current for evoking the EEPs in group 3 was 400 ± 0 μA before the retinectomy and 400 ± 0 μA after the retinectomy. The means ± SDs of the amplitude and implicit times of EEPs elicited by 1000, 750, 500, and 400 μA are shown in Figures 3F1 and 3F2. There was no significant difference in the amplitude and the implicit times of EEPs before and after retinectomy ($P = 0.058$–0.716). Thus, removing the nonirra-

diated retina from the degenerated retina and optic nerve did not reduce the EEPs.

DISCUSSION

In a pilot study, we irradiated eyes with stronger light and for longer durations (24 hours) without verteporfin and failed to damage large areas of the outer retinal layer. We, therefore, used verteporfin according to a report on the predominant damage of the outer retinal layer by repeated PDT.[17] We also chose a red LED for the light source because the LED light does not generate heat as easily as do other light sources, and 630 nm is the peak excitation wavelength of verteporfin.[20,21]

We then conducted another pilot study to develop a retinal degeneration model with verteporfin and a red LED. We changed the dose of verteporfin (0.24, 0.47, and 0.96 mg/kg), total irradiation time (45 and 90 minutes), irradiation direction (1 and 3 directions) and distance (0 and 15 mm), and finally succeeded in creating substantial damage to the outer retinal layers with a dose of 0.47 mg/kg verteporfin and irradiation from 3 directions for 30 minutes, each when the red LED was placed just in front of the diffuser contact lens. These conditions induced retinal degeneration in which the outer retinal layers were preferentially damaged and the inner retinal layers were relatively well preserved. In addition, the damage was extensive and uniform. We conclude that our technique of photochemical damage with verteporfin and a red LED light can produce retinal degeneration resembling the histologic characteristics of eyes of patients with RP.

The amplitudes of the full-field ERGs remained about one half that of the controls (Figs. 2A, 2B) because the degenerated region did not cover the entire retina (Figs. 1A-F). In contrast, focal ERGs were not elicited when the stimulus spot was placed on the degenerated area (Fig. 2C). This result corresponded with the histologic findings that the outer retinal layers were almost completely absent in the irradiated area (Figs. 1G-L). However, the inner retinal layers were somewhat intact in the damaged region, which is known to be characteristic of the end stage of human RP.[2] These results demonstrated that the damaged region of this model resembled the

A

control

1 month

100 μV

30 msec

B

	Control	Post-1M	P Value
Amplitude(μV)			
a-wave	68.8±24.7	33.6 ±8.8	**P^*=0.016**
b-wave	203.8 ±85.2	108.7±24.1	**P^*=0.008**
Implicit time(ms)			
a-wave	11.2±0.6	10.7±1.2	P^*=0.548
b-wave	39.4 ±4.4	34.2±6.0	P^*=0.095

C

5Hz

30Hz

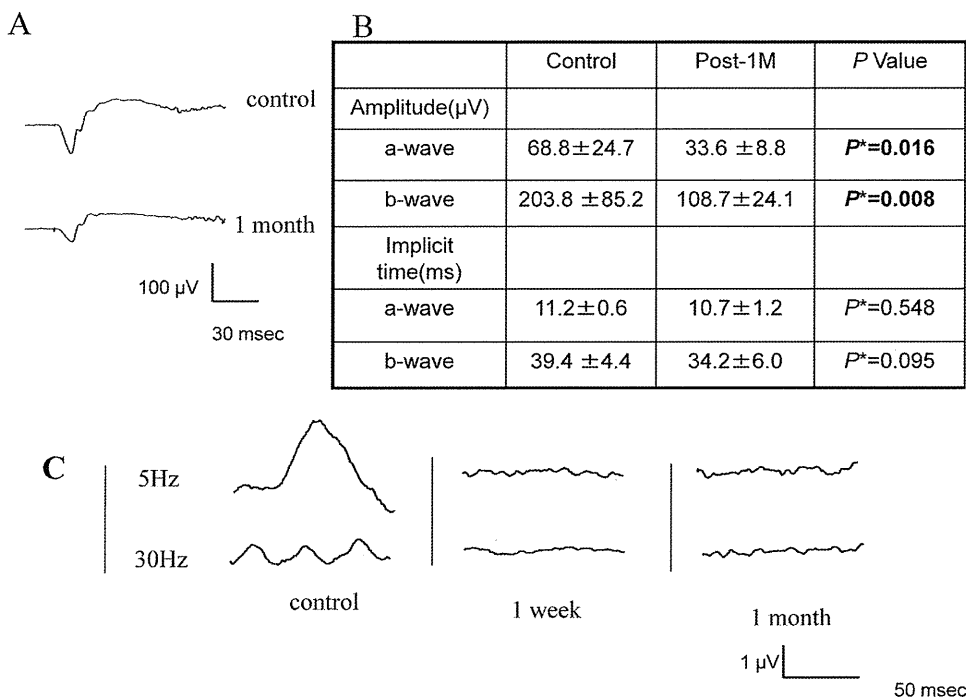control   1 week   1 month

1 μV

50 msec

FIGURE 2. Representative full-field (A) and focal (C) ERGs at 1 month after irradiation. The amplitudes of the a- and b-waves at 1 month were reduced to one half of the control value (B). Data are shown as the means ± SD. *Mann-Whitney rank sum test with significant differences in *bold.*
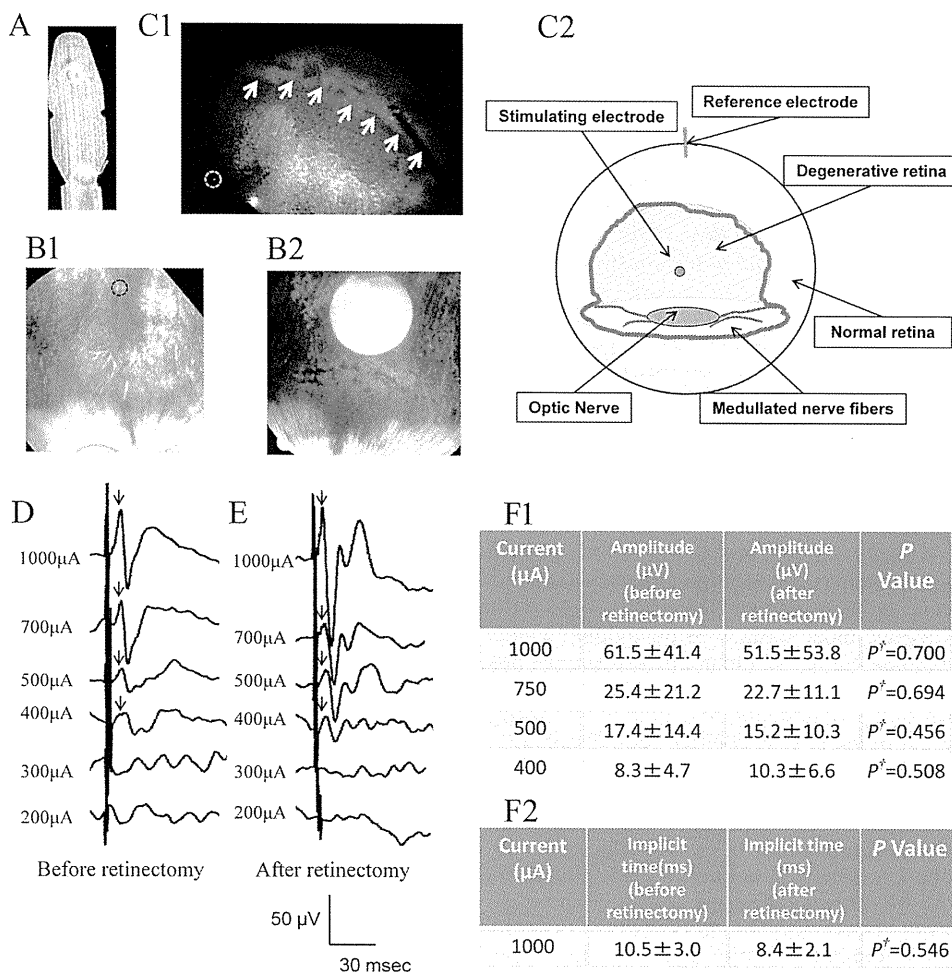
F1

Current (μA)	Amplitude (μV) (before retinectomy)	Amplitude (μV) (after retinectomy)	P Value
1000	61.5±41.4	51.5±53.8	P^*=0.700
750	25.4±21.2	22.7±11.1	P^*=0.694
500	17.4±14.4	15.2±10.3	P^*=0.456
400	8.3±4.7	10.3±6.6	P^*=0.508

F2

Current (μA)	Implicit time(ms) (before retinectomy)	Implicit time (ms) (after retinectomy)	P Value
1000	10.5±3.0	8.4±2.1	P^*=0.546
750	11.7±4.7	12.9±4.8	P^*=0.716
500	12.2±5.1	11.0±5.8	P^*=0.339
400	14.0±5.8	11.4±6.0	P^*=0.058

FIGURE 3. Inserted STS electrode and isolated degenerated retina and representative EEPs. (**A**) STS electrode (diameter 500 μm) inserted in the degenerated area (**B1**, *dotted black outline*) was apparently smaller than the photic stimuli for focal ERGs (**B2**). Retinectomy was performed (**C1**, *white arrows*) along the border of the degenerative retina and normal retina (**C2**, *red line*); inserted STS electrode (**C1**, *dotted white outline*) and representative EEPs (*black arrows*) before (**D**) and after retinectomy (**E**). The amplitudes (**F1**) and the implicit times (**F2**) of the EEPs after retinectomy were not significantly different from those before the retinectomy. Data are the mean ± SD. †Paired *t*-tests.

histologic and physiological characteristics of eyes of patients with RP.

Despite the absence of focal ERGs when the stimulus was placed on the damaged area (Fig. 2C), EEPs could still be elicited by the STS electrode placed beneath the irradiated area (Figs. 1N, 3B1, 3B2). These results indicate that the STS electrode can stimulate the inner retina in the area that has been damaged by the irradiation to evoke EEPs. One year after irradiation, the ONL had entirely disappeared, and even the INL was significantly decreased but partially remained as shown in the histologic sections (Fig. 1L, Table 1).

Because the EEPs are evoked from ganglion cells and partly from bipolar cells, even though the ONL was completely absent, the EEPs at 1 year after the irradiation were not significantly different from those recorded 1 month after the irradiation.

However, the EEPs may have been evoked by stray currents that stimulated functioning neurons some distance from the irradiated area. To eliminate this possibility, we removed the normal retina surrounding the degenerated area by retinectomy. Our findings showed that EEPs of the same amplitude and thresholds could still be elicited. Thus, we conclude that the EEPs were not elicited by stray currents (Figs. 3C–F). In addition, these findings demonstrate that the degenerated area with our parameters of photocoagulation was large enough to evaluate the effect of the STS system.

The shapes of the EEPs in our rabbits were different from those of RCD1,[22,23] which may be because of the differences in retinal prosthesis, the number of stimulating electrodes, and the current densities.

Earlier studies[24–33] reported that an intravenous administration of either monoiodoacetic acid (IAA) or sodium iodate (NaIO₃) can damage the retina. IAA is well known to be retinotoxic and to damage the photoreceptors selectively,[25–27] and the damage of the inner retinal layer is much less severe than that of the outer retinal layers.[24,28] However, the effect of this toxin is uneven among individuals and occasionally even between the eyes of the same animal.[28] Liang et al.[28] injected IAA intravenously at a dose of 20 mg/kg into 23 rabbits and found a uniformly decreased ONL in only 3 eyes, partial damage of the ONL in 9 eyes, and no change in 11 (48%) eyes. Because a dose of 20 mg/kg IAA is relatively high and results in a high mortality (20%),[29] increasing the dose of this drug to damage the ONL more uniformly is not practical. Our method has the advantages that a predominant outer retinal degeneration can be created with almost 100% certainty.

There are many reports[30–33] on the NaIO₃-induced retinal degeneration. Sorsby[31] injected different concentrations of NaIO₃ (10–60 mg/kg) into rabbits intravenously and concluded that an incidence of 100% of retinal lesions was attained at a dose of 25 mg/kg. But he did not evaluate the size of the lesions. In another study[32] an injection of NaIO₃ at a dose of 25

mg/kg into rabbits intravenously caused patchy RPE degeneration and photoreceptor degeneration.

Injection of $NaIO_3$ at a dose of 40 mg/kg which is the most commonly used concentration for functional evaluations of retinal prostheses[24,33] caused apoptosis in the photoreceptor layer and in the INL at 1 week after the injection and apoptosis in the GCL at 3 weeks. A severe apoptosis of the GCL was noted 4 months after the injection.[33] In another study,[24] an injection of $NaIO_3$ at a dose of 40 mg/kg led to a reduction of 76% in the a-wave and of 67% in the b-wave amplitudes of the control subjects.

In contrast to $NaIO_3$, the retinal degeneration of our model was limited and uniform and large enough for a functional evaluation of a retinal prosthesis. Our model at 1 year (group 2) showed that the cell counts in the GCL were not significantly different ($P = 0.903$; Table 1). More important, we were able to elicit EEPs by STS electrode at 1 year after the irradiation (Fig. 1O). Thus, our model can be used as a retinal degenerative model for testing retinal prostheses for at least 1 year after irradiation.

A recent study[34] demonstrated that phased tissue remodeling and functional reprogramming of the neural retina may occur in degenerative diseases such as retinitis pigmentosa. However, most studies on developing a degenerative model including our model did not investigate the possibility of neural reprogramming, and more investigations are needed to confirm tissue remodeling and functional reprogramming of the neural retina in degenerative retinal models.

In conclusion, we succeeded in developing a middle-sized animal model of photoreceptor degeneration. Our model will help to determine the optimal stimulus parameter to elicit EEPs in degenerated retinas by STS electrode. In addition, these parameters may be helpful to elicit phosphenes from patients with RP. This middle-sized animal model is easy to handle and to be created, and should be helpful to evaluate not only the STS system but also other types of retinal prostheses including subretinal and epiretinal stimulations.

References

1. Stone JL, Barlow WE, Humayun MS, et al. Morphometric analysis of macular photoreceptors and ganglion cells in retinas with retinitis pigmentosa. Arch Ophthalmol. 1992;110:1634–1639.

2. Santos A, Humayun MS, de Juan E Jr, et al. Preservation of the inner retina in retinitis pigmentosa: a morphometric analysis. Arch Ophthalmol. 1997;115:511–515.

3. Chow AY, Chow VY, Packo KH, at al. The artificial silicon retina microchip for the treatment of vision loss from retinitis pigmentosa. Arch Ophthalmol. 2004;122:460–469.

4. Humayun MS, Weiland JD, Fujii GY, et al. Visual perception in a blind subject with a chronic microelectronic retinal prosthesis. Vision Res. 2003;43:2573–2581.

5. Rizzo JF 3rd, Wyatt J, Loewenstein J, et al. Methods and perceptual thresholds for short-term electrical stimulation of human retina with microelectrode arrays. Invest Ophthalmol Vis Sci. 2003;44:5355–5361.

6. Zrenner E. The subretinal implant: can microphotodiode arrays replace degenerated retinal photoreceptors to restore vision? Ophthalmologica. 2002;216(suppl 1):8–20.

7. Sakaguchi H, Kamei M, Fujikado T, et al. Artificial vision by direct optic nerve electrode (AV-DONE) implantation in a blind patient with retinitis pigmentosa. J Artif Organs. 2009;12(3):206–209.

8. Fujikado T, Morimoto T, Kanda H, et al. Evaluation of phosphenes elicited by extraocular stimulation in normals and by suprachoroidal-transretinal stimulation in patients with retinitis pigmentosa. Graefes Arch Clin Exp Ophthalmol. 2007;245:1411–1419.

9. Sakaguchi H, Fujikado T, Fang X, et al. Transretinal electrical stimulation with a suprachoroidal multichannel electrode in rabbit eyes. Jpn J Ophthalmol. 2004;48:256–261.

10. Nakauchi K, Fujikado T, Kanda H, et al. Transretinal electrical stimulation by an intrascleral multichannel electrode array in rabbit eyes. Graefes Arch Clin Exp Ophthalmol. 2005;243:169–174.

11. Kanda H, Morimoto T, Fujikado T, et al. Electrophysiological studies of the feasibility of suprachoroidal-transretinal stimulation for artificial vision in normal and RCS rats. Invest Ophthalmol Vis Sci. 2004;45:560–566.

12. LaVail MM. Legacy of the RCS rat: impact of a seminal study on retinal cell biology and retinal degenerative diseases. Prog Brain Res. 2001;131:617–627.

13. Machida S, Kondo M, Jamison JA, et al. P23H rhodopsin transgenic rat: correlation of retinal function with histopathology. Invest Ophthalmol Vis Sci. 2000;41:3200–3209.

14. Ray K, Baldwin VJ, Acland GM, et al. Cosegregation of codon 807 mutation of the canine rod cGMP phosphodiesterase beta gene and rcd1. Invest Ophthalmol Vis Sci. 1994;35:4291–4299.

15. Acland GM, Fletcher RT, Gentleman S, et al. Non-allelism of three genes (rcd1, rcd2 and erd) for early onset hereditary retinal degeneration. Exp Eye Res. 1989;49:983–998.

16. Kijas JW, Cideciyan AV, Aleman TS, et al. Naturally occurring rhodopsin mutation in the dog causes retinal dysfunction and degeneration mimicking human dominant retinitis pigmentosa. Proc Natl Acad Sci USA. 2002;99:6328–6333.

17. Reinke MH, Canakis C, Husain D, et al. Verteporfin photodynamic therapy retreatment of normal retina and choroid in the cynomolgus monkey. Ophthalmology. 1999;106:1915–1923.

18. Miyake Y, Shiroyama N, Ota I, et al. Oscillatory potentials in electroretinograms of the human macular region. Invest Ophthalmol Vis Sci. 1988;29:1631–1635.

19. Kondo M, Ueno S, Piao CH, et al. Comparison of focal macular cone ERGs in complete-type congenital stationary night blindness and APB-treated monkeys. Vision Res. 2008;48:273–280.

20. Tsoukas MM, Lin GC, Lee MS, et al. Predictive dosimetry for threshold phototoxicity in photodynamic therapy on normal skin: red wavelengths produce more extensive damage than blue at equal threshold doses. J Invest Dermatol. 1997;108:501–505.

21. Waterfield EM, Renke ME, Smits CB, et al. Wavelength-dependent effects of benzoporphyrin derivative monoacid ring A in vivo and in vitro. Photochem Photobiol. 1994;60:383–387.

22. Guven D, Weiland JD, Fujii G, et al. Long-term stimulation by active epiretinal implants in normal and RCD1 dogs. J Neural Eng. 2005;2(1):S65–S73.

23. Chen SJ, Mahadevappa M, Roizenblatt R, et al. Neural responses elicited by electrical stimulation of the retina. Trans Am Ophthalmol Soc. 2006;104:252–259.

24. Humayun M, Sato Y, Propst R, et al. Can potentials from the visual cortex be elicited electrically despite severe retinal degeneration and a markedly reduced electroretinogram? Ger J Ophthalmol. 1995;4(1):57–64.

25. Noell WK. The impairment of visual cell structure by iodoacetate. J Cell Physiol. 1952;40:25–55.

26. Lasansky A, Robertis E. Submicroscopic changes in visual cells of the rabbit induced by iodoacetate. J Biophysic Biochem Cytol. 1959;5(2):245–250.

27. Noell WK. Some animal models of retinitis pigmentosa. Adv Exp Med Biol. 1977;77:87–91.

28. Liang L, Katagiri Y, Franco LM, et al. Long-term cellular and regional specificity of the photoreceptor toxin, iodoacetic acid (IAA), in the rabbit retina. Vis Neurosci. 2008;25:167–177.

29. Orzalesi N, Calabria GA, Grignolo A. Experimental degeneration of the rabbit retina induced by iodoacetic acid: a study of the ultrastructure, the rhodopsin cycle and the uptake of 14C-labeled iodoacetic acid. Exp Eye Res. 1970;9(2):246–253.

30. Noell WK. Metabolic injures of the visual cell. Am J Ophthalmol. 1955;40(2):60–70.

31. Sorsby A. Experimental degeneration of the retina, IX: fasting as a potentiating factor. Vision Res. 1962;2:157–162.

32. Korte GE, Reppucci V, Henkind P. RPE destruction causes choriocapillary atrophy. Invest Ophthalmol Vis Sci. 1984;25:1135–1145.

33. Wang K, Li XX, Jiang YR, et al. Influential factors of thresholds for electrically evoked potentials elicited by intraorbital electrical stimulation of the optic nerve in rabbit eyes. Vision Res. 2007;47:3012–3024.

34. Marc RE, Jones BW, Watt CB, et al. Neural reprogramming in retinal degeneration. Invest Ophthalmol Vis Sci. 2007;48:3364–3371.

ORIGINAL RESEARCH

Detection of photoreceptor disruption by adaptive optics fundus imaging and Fourier-domain optical coherence tomography in eyes with occult macular dystrophy

Yoshiyuki Kitaguchi[1]
Shunji Kusaka[1]
Tatsuo Yamaguchi[2]
Toshifumi Mihashi[2]
Takashi Fujikado[1]

[1]Department of Applied Visual Science, Osaka University Graduate School of Medicine, Osaka, Japan; [2]Topcon Research Institute, Itabashi, Japan

Purpose: To investigate the structural changes in the photoreceptors by adaptive optics (AO) fundus imaging and Fourier-domain optical coherence tomography (FD-OCT) in eyes with occult macular dystrophy (OMD).

Design: Observational case reports.

Methods: Eight eyes of four patients who were diagnosed with OMD were examined. All eyes had a complete ophthalmological examination. Multifocal electroretinograms (mfERGs) were recorded from all eyes. AO and FD-OCT images of foveal photoreceptors were obtained.

Results: The best-corrected visual acuity (BCVA) of these eyes ranged from 20/20 to 20/200, and the ocular fundus was normal by conventional ocular examination in all eyes. The amplitudes of the mfERGs were decreased in the foveal area. The inner and outer segment (IS/OS) junction of the photoreceptors in the foveal area was disrupted. The IS/OS junction was intact in one eye with a BCVA of 20/20, and the outer segment layer between the IS/OS junction and retinal pigment epithelium of the FD-OCT images was identified only in the center of the fovea. The AO images showed patchy dark areas in all eyes, which indicated a disruption of the mosaic of bright spots in the fovea.

Conclusion: Structural changes of photoreceptors in OMD patients were detected tangentially by FD-OCT and en face by AO.

Keywords: Photoreceptors, OMD, images, retinal imaging

Introduction

Occult macular dystrophy (OMD) is a progressive hereditary macular dystrophy which is characterized by reduced visual acuity with an essentially normal fundus and normal fluorescein angiography.[1] Full-field electroretinograms (ERGs) are normal in OMD patients, and only the focal macular ERGs and multifocal ERGs (mfERGs) recorded from the macular area are reduced.[2,3]

With advances in retinal imaging, it has become easier to detect anatomical changes of the retina in eyes with OMD. Thus, Kondo et al reported a reduction of the retinal foveal thickness measured by time domain optical coherence tomography (OCT) in OMD patients,[4] and Brockhurst et al reported a thinning of the outer nuclear layer that was measured by Stratus OCT in OMD patients.[5] Although the main site of the lesion appeared to be the photoreceptor layer, abnormalities of the photoreceptors have not been reported in imaging studies. This deficiency is probably because of the low axial and transverse resolution of the imaging instruments.

Correspondence: Takashi Fujikado
Department of Applied Visual Science,
Osaka University Graduate School of
Medicine, 2-2 Yamadaoka, Suita, Osaka
565-0871, Japan
Tel +81 6 6879 3941
Email fujikado@ophthal.med.osaka-u.ac.jp

1

The axial resolution of the Fourier-domain OCT (FD-OCT) is approximately 6 μm, which is significantly better than the 10 μm of standard OCTs. The external limiting membrane (ELM) (first highly reflective line), photoreceptor inner and outer segment junction (IS/OS) (second line), and the retinal pigment epithelium (RPE) (fourth line) can all be detected with an FD-OCT.[6–9] Disturbances of the IS/OS junction have been reported in some retinal diseases, eg, postoperative retinal detachment, central serous chorioretinopathy, and retinal dystrophy, which could not be detected ophthalmoscopically.[7,10–13] A disruption of the third highly reflective line of the FD-OCT images has been reported in cases of macular microhole.[13] Because the third line is considered to represent the outer segment of the photoreceptors because of its anatomical position, the disruption suggests an alteration of the photoreceptor outer segments. However, the origin of the third line has not been well investigated.

The adaptive optics (AO) fundus camera can obtain images with a transverse resolution of <2 μm, which makes it possible to resolve individual photoreceptors in living human eyes.[14–20] An increase in the cone spacing in retinas with cone dystrophy can be detected by AO imaging,[20,21] and the degree of the increased spacing is consistent with the decrease in visual function measured by mfERGs.[20] A disruption of the third bright line of the FD-OCT images is reported to cause a dark area in the AO fundus images.[14,15]

The purpose of this study was to determine whether the photoreceptor abnormalities in eyes with OMD can be detected tangentially in the FD-OCT images and en face in the AO fundus images.

Subjects and methods
Subjects

Eight eyes of four patients, who were diagnosed with OMD in the Department of Ophthalmology, Osaka University School of Medicine, were studied. The diagnosis of OMD was made by the following findings: normal fundus, normal fluorescein angiography, decreased visual acuity, normal full-field ERGs for both rod and cone components, and reduced amplitude of mfERGs in the central 5 degrees. All of the patients were classified as having sporadic OMD because none reported other family members with similar visual problems. Some of the characteristics of these OMD patients are summarized in Table 1.

The research protocol was approved by the Institutional Review Board of the Osaka University Medical School, and the procedures used conformed to the tenets of the Declaration of Helsinki. After the nature and possible consequences

Table I Clinical characteristics of examined patients

Age	Sex	Eye	Visual acuity	Spherical equivalent (D)	Progression	Scotoma size	Fundus	Full-field ERGs	OCT findings IS/OS	OCT findings OS
48	M	Right	20/100	−0.25	3 years	None	Normal	Normal	Severely disrupted	−
		Left	20/66	0		Central 10 deg	Normal	Normal	Severely disrupted	−
38	M	Right	20/66	−6.25	Unknown	Perifoveal 2.5 deg	Normal	Normal	Severely disrupted	−
		Left	20/66	−6		Central 3 deg	Normal	Normal	Severely disrupted	−
46	F	Right	10/100	−2.5	6 months	Central 2.5 deg	Normal	Normal	Disrupted in fovea	+
		Left	20/20	−1.75		None	Normal	Normal	Almost normal	+
43	M	Right	20/100	−1.75	18 years	Central 2.5 deg	Normal	Normal	Severely disrupted	−
		Left	20/100	−1.75		Central 2.5 deg	Normal	Normal	Disrupted	−

Abbreviations: ERG, electroretinogram; F, female; IS, inner segment; M, male; OCT, optical coherence tomography; OS, outer segment.

of the study were explained, a written informed consent was obtained from all patients.

The mfERGs were recorded with the Veris Clinic system (Mayo Co., Aichi, Japan) under standardized conditions. The stimulus array consisted of 103 hexagons, and the luminance of each hexagon was alternated between 200 cd/m² and 5 cd/m². A cross sectional image of the retina was obtained by a FD-OCT (RTVue-100; Optovue Inc., Fremont, CA). Horizontal and vertical scans were made through the fovea with a scan length of 6 mm. To improve the signal-to-noise ratio, consecutive images were averaged with the built-in software.

AO fundus images

The AO fundus images were taken through pupils dilated with topical tropicamide (0.5%) and phenylephrine (0.5) and the ciliary muscle paralyzed. A detailed description of the custom-built AO fundus camera has been published,[23,24] and the principle of our flood illumination AO fundus camera is similar to that reported by Roorda and Williams.[15] Briefly, the main components of the camera were a nematic liquid crystal phase modulator (LCPM: X8267-12; Hamamatsu Photonics, Hamamatsu, Japan), a Hartmann-Shack wavefront sensor (HSWS: 28 × 28 lenslets; specially made by Topcon, Co., Tokyo, Japan), and a scientific CCD digital camera (C9100-02; Hamamatsu Photonics, Hamamatsu, Japan). The wavefront sensor measured the ocular wavefront up to the eighth Zernike order, and the phase modulator compensated for the measured wavefront aberrations. The system is also equipped with coaxial, 8-degree-wide viewing optics to identify the location and orientation of the highly magnified retinal images.

The retina was illuminated with a 2-ms flash (635-nm wavelength) from a laser diode, and a retinal image was obtained with a 6-mm diameter exit pupil. The patient was instructed to fixate a target in the center of the field. Frame-averaging was performed using custom software (Topcon) to improve the quality of the image. Overlapping images were merged using Photoshop (Adobe Systems Inc., San Jose, CA).

Results

The age of the patients ranged from 38 to 48 years. The best-corrected visual acuity (BCVA) at examination ranged from 20/200 to 20/20. None of the patients had an episode of sudden loss of visual acuity. The duration of decrease of vision ranged from 3 months to 3 years; six eyes out of eight had a central relative scotoma by Goldmann perimetry.

Multifocal ERGs

The amplitudes of the mfERGs in the central area were reduced in all eyes. The area of the decreased amplitude varied among eyes (Figure 1).

FD-OCT

All eyes showed a disruption of the IS/OS line except the left eye of patient 3 who had a visual acuity of 20/20; meanwhile the IS/OS line and the third line are easily identifiable in normal control. Both eyes of patients 1 and 2 had a severe disruption of IS/OS line in the center of the fovea, and both had a low-intensity space between the elevated
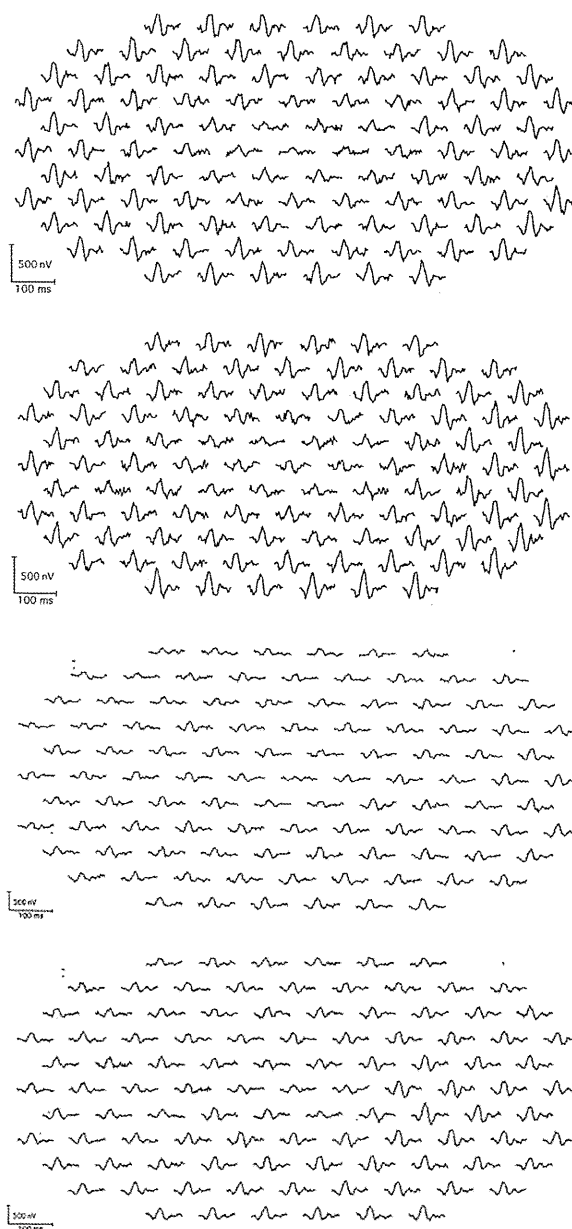

Figure 1 (*Continued*)